

Biological Report 11  
April 1993

# **In-water Electrical Measurements for Evaluating Electrofishing Systems**

By

A. Lawrence Kolz

U.S. Department of the Interior  
Fish and Wildlife Service  
Washington, D.C. 20240



# Contents

	Page
Abstract . . . . .	1
Measurement of Electrode Resistance . . . . .	2
Electrical Theory . . . . .	2
Measurement Procedures . . . . .	3
Effects of Water Conductivity . . . . .	4
Measured Resistance Values for Metal Cylinders . . . . .	4
Circuit Analysis Techniques for Electrode Arrays . . . . .	4
Resistance Analysis . . . . .	5
Voltage and Current Analysis . . . . .	5
Power Analysis . . . . .	6
Comments on Power Supply Instrumentation . . . . .	6
Voltage Measurements in a Volume of Water . . . . .	6
Quasi-technical Concepts for Electric Fields in Water . . . . .	7
In-water Voltage Measurement Techniques . . . . .	8
Test Procedures . . . . .	11
Description of the Test Electrodes . . . . .	11
Measurement Site and Techniques . . . . .	11
Presentation of In-water Electrode Measurements . . . . .	12
Values of Electrode Resistance . . . . .	12
Spatial Comparisons of Electric Fields . . . . .	13
Voltage Profiles . . . . .	13
Voltage Gradient Profiles . . . . .	15
Discussion of the Voltage Gradient Vector . . . . .	17
Discussion . . . . .	21
Acknowledgments . . . . .	22
References . . . . .	22
Appendix. Glossary of Electrical Terms. . . . .	24



# In-water Electrical Measurements for Evaluating Electrofishing Systems

by

A. Lawrence Kolz

*U.S. Department of Agriculture  
Denver Wildlife Research Center  
Animal and Plant Health Inspection Service  
Denver Federal Center, Building 16  
Denver, Colorado 80225*

**Abstract.** The design of electrodes for electrofishing equipment is developed using in-water electrical measurements that apply to any electrode configuration, and the measurement techniques require only common, inexpensive electrical meters that are readily available to field biologists. Circuit analysis techniques are described for determining the voltage, current, and power requirements for an electrofishing system, and the relation between water conductivity and electrode resistance is demonstrated. Electrode resistance values, voltage profiles, voltage gradient profiles, and comparative indices are presented for 18 common electrodes. The fallacy of monitoring voltage, current, or power as a standardization procedure for electrofishing equipment is discussed in detail.

**Key words:** Anode, cathode, electrical shock, electricity, electrode, electrofishing, fish, voltage gradient.

Electrofishing systems, designed for the capture or control of fish, induce electrical power into the water with submerged metal electrodes. These electrodes function as metal-to-water transducers and provide the interface between the power supply and the water. At least two electrodes are necessary to complete an electrical circuit through water, but electrofishing systems are often electrified with multiple electrodes (Novotny and Priegel 1974). These arrays of electrodes provide additional contacts with the water and alter the size and power density of the resultant electric field. Electrode arrays usually increase a system's area of coverage and enhance operating efficiency. Field personnel should be capable of modifying their electrodes to optimize the performance of their electrofishing equipment for the prevailing conditions and to compare the operating characteristics. I present technical information, measurement techniques, and comparative data to assist in the design of these electrodes.

Within the past decade, fishery biologists have attempted to monitor and manage fish populations based on indices developed from electrofishing methodologies. These seasonal and time-repetitive surveys demand standardized collection methods (Heidinger et al. 1983; Wiley and Tsai 1983), which require that consistent and comparable electrical parameters be adapted for the sampling. Obviously, one would not expect to seine an equal number of fish with different size nets, and the same is true when electrofishing with dissimilar electric fields. Unfortunately, it is a common error to judge the electrical fields for two electrofishing apparatus as being operationally similar based on comparative voltage, current, or power readings at the generator or equipment control panel. The voltage and current controls actually adjust the power being applied into the water, but they do not uniquely determine the intensity of the resulting electric field. Researchers must understand that fish are electroshocked by the distribution and intensity of the electrical energy in the water (Kolz

and Reynolds 1989), and the spatial characteristics of this energy are determined by a combination of factors including the applied power, electrode configuration, and water conductivity. The effectiveness of any particular electrofishing unit can be changed significantly simply by modifying the electrodes even though the same measured voltage, current, or power may be applied. These differences occur because the geometric configurations of the individual electrodes in combination with their placement in the water define the shape, size, and distribution of the electrical power in the volume of water. For field operations, the electrical power can never be uniformly distributed in the water (Seidel and Klima 1974), and it becomes imperative to understand how the power is distributed or concentrated near the electrodes.

Studies of electric fields involve advanced engineering concepts, higher level mathematics, and the use of uncommon electrical terms. Biologists, whose only intent is to have a practical working knowledge of their equipment, may be discouraged by this degree of technical sophistication. Unfortunately, it is not possible to circumvent the technical jargon, but I describe procedures that will allow field biologists to actually measure and adequately design electrodes with common, inexpensive instruments. The terminology, symbols, and equations, as presented by Kolz (1989), are summarized in the Appendix.

There are always two electrical barriers to interface when electroshocking fish. First, the electrical power must transfer from the electrodes into the water, and then, the power must transfer from the water into the fish. The singular concern addressed in this paper is the electrical power transfer from the metal electrodes into the water; no consideration is given to the mechanism of energy transfer into the fish (see Kolz and Reynolds 1989). Biologists can use this information to design, evaluate, adjust, and compare the characteristics of electrodes. Four aspects of electrode design are discussed: (1) measurements for determining electrode resistance, (2) circuit analyses of electrode arrays, (3) in-water voltage measurements, and (4) comparative data for specific electrode configurations.

All electrodes are assumed to be constructed with clean, smooth, high-conductivity metals without surface contamination or corrosion; no distinction is made between metals. DeMont (1971) compared the advantages of using specific metals in the construction of electrofishing elec-

trodes. In practice, aluminum electrodes are popular because of the variety of configurations available at low cost, but stainless steel is recognized as being more durable.

## Measurement of Electrode Resistance

The procedures necessary to measure electrode resistance in water are developed from basic circuit theory, and the experimental techniques apply to any size or shape of electrode. This empirical method contrasts with the theoretical approach that is limited to only a few electrode configurations having known mathematic or graphic solutions (Novotny and Priegel 1974). Also, the book solutions often impose boundary conditions that are impractical for field applications and cause significant errors in the calculated values of electrode resistance.

### *Electrical Theory*

Electrofishing systems all require a power source and a minimum of two electrodes. The two electrodes form a series circuit (Fig. 1). The electrodes can be treated in any analysis as discrete circuit components, and the total circuit resistance is the sum of the individual electrode resistances expressed in ohms. Thus,

$$R(\text{total}) = R(\text{electrode 1}) + R(\text{electrode 2}) \text{ ohms.} \quad (1)$$

In other words, standard circuit analysis techniques apply to electrofishing electrodes because a

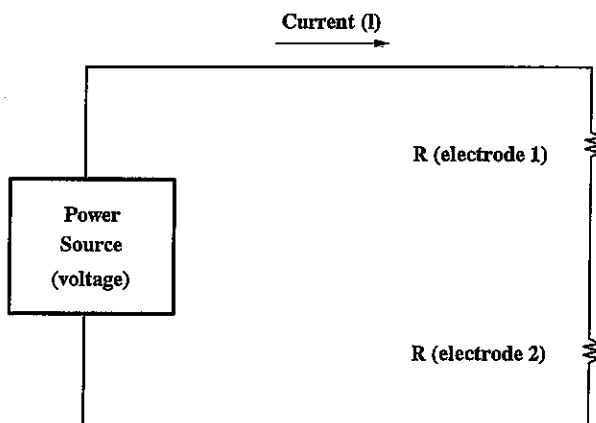


Fig. 1. Basic electrical circuit for electrofishing equipment.

net value of resistance can be associated with every electrode.

If two electrodes are constructed physically identical, they will also be electrically similar and exhibit the same value of electrode resistance. The total circuit resistance for two similar electrodes is then twice the value of a single electrode expressed in ohms. Hence,

$$R(\text{total}) = 2 \times R(\text{individual electrode}) \text{ ohms.} \quad (2)$$

### Measurement Procedures

The following procedures will determine the resistance for an electrode. These measurements may be conducted at any test site (lake, river, swimming pool, irrigation canal, etc.) judged realistic for the anticipated operational situation.

1. Construct two identical electrodes or electrode arrays.
2. Immerse the electrodes in water to their intended operational depth. Be aware that the depth of water, the separation distance, and the surrounding substrate can alter the results.
3. Connect a power source of alternating current (AC) with appropriate multimeters (high impedance, analog or digital volt-ohm-amp meters) to measure the volts (V) and amperes (A) as shown in Fig. 2. If a grounded electrical source is used (e.g., household 120 volts AC), it is advisable to use an isolation transformer for the safety of personnel and the prevention of unwanted leakage currents. The AC generators used to power electrofishing boats can also be used as an electrical supply, and since these generators are normally operated with the neutral electrical connection removed (this isolates the generator frame and boat hull from the power circuit), there is no need for an isolation transformer.
4. With power applied to the electrodes, increase the separation between the electrodes and note if the current changes. A significant variation in current indicates interspatial coupling between the two electrode fields; the electrodes are not isolated and operating independently. It is usually desirable to measure electrodes having isolated electric fields.
5. To ensure isolation, separate the electrodes to a distance where the ammeter readings stabilize before recording the current and volts. It is not necessary to belabor this separation procedure because small variations in the current do not significantly change the results.

6. Apply Ohm's Law to calculate the total circuit resistance:

$$R(\text{total}) = V(\text{volts}) / I(\text{A}) \text{ ohms.}$$

7. Apply equation 2 to calculate the resistance of a single electrode:

$$R(\text{individual electrode}) = R(\text{total}) / 2 \text{ ohms.}$$

8. Record the electrical conductivity of the water.

The above procedures specify an AC power source. Actually, other voltage waveforms can be used to measure electrodes if precautions are taken regarding the instrumentation. The resistance of an electrode is not changed by the applied waveform: the resistance is the same for AC, direct current (DC), pulsed direct current (PDC), or pulsed alternating current (PAC). The concern when making an electrical measurement is that the common multimeters are only designed to provide correct readings with continuous DC or sinusoidal AC waveforms. Pulsed direct current or nonsinusoidal AC waveforms require special instruments. Additionally, DC measurements present an uncommon problem. Conway (1965) described an unstable electrical phenomenon known as the Helmholtz effect when DC voltages are applied to metal electrodes, but the Helmholtz effect is avoided by using AC.

Caution is advised when making resistance measurements in static water. Electrolysis forms gas bubbles around the electrodes, and the surface of an electrode can become partially insulated. This effect is minimized by quickly recording the voltage and current before many bubbles adhere to the surface. Under field conditions, these gas by-

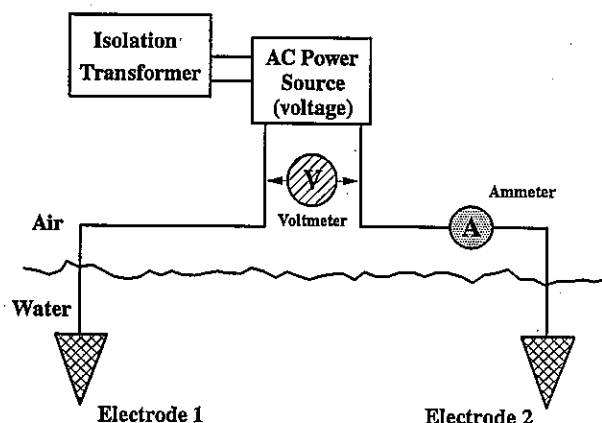


Fig. 2. Circuit configuration with metering for measuring electrode resistance.

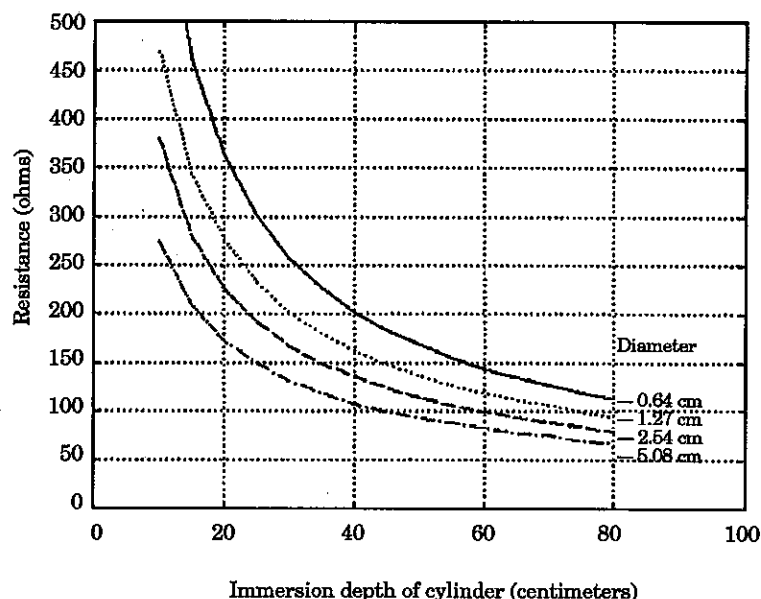


Fig. 3. Individual electrode resistance values for cylinders in water having a conductivity of 100  $\mu\text{S}/\text{cm}$ .

products are swept away by the movement of the electrodes through the water.

### *Effects of Water Conductivity*

The measurement procedures determine an electrode's resistance for a specific value of water conductivity. When the electrode is submerged into water having a different conductivity, the electrode's resistance will change in inverse proportion to the two values of water conductivity. That is,

$$R_2 / R_1 = c_1 / c_2 \quad (3)$$

where  $R_2$  is the resistance of the electrode in the water having a conductivity equal to  $c_2$ , and  $R_1$  is the resistance of the electrode in the original water having a conductivity of  $c_1$ . Therefore, the resistance of an electrode can be calculated for any value of water conductivity once its resistance is experimentally determined for water of known conductivity.

### *Measured Resistance Values for Metal Cylinders*

Figure 3 presents electrode resistance measurements for individual cylinders having outside diameters of 0.64, 1.27, 2.54, and 5.08 cm when suspended vertically to submerged cylinder lengths ranging from 15 to 80 cm in water having a conductivity of 100 microsiemens/cm ( $\mu\text{S}/\text{cm}$ ). For a cylinder length of 15 cm, these empirical results were almost 100% less than the theoretical

estimations (Novotny and Priegel 1974), and this difference decreases to less than 50% with cylinder lengths of 80 cm. This error is predictable because the theoretical solution neglects the distortion created in the electrical field by the current conducted from the ends of the cylinders. This distortion becomes less significant as the cylinder length is increased. However, the magnitude of the error is more than might be anticipated for such a simple electrode and indicates why an experimental approach is desirable and necessary for complex electrode configurations.

## **Circuit Analysis Techniques for Electrode Arrays**

Commercially manufactured electrofishing apparatuses from the United States are designed as single phase, two-terminal systems. An electrode is wired to each of the two terminals of the power source via interconnecting electrical lines or leads. Often, additional electrodes are connected to either or both terminals of the power source to create an array of multiple electrodes. Every electrode attached to a given line is electrically connected in parallel with all other electrodes attached to the same line. The generic circuit for a two-terminal system having multiple electrodes is depicted in Fig. 4a for "M" electrodes attached to line A and "N" electrodes to line B. The series connection between the two parallel circuits (i.e.,



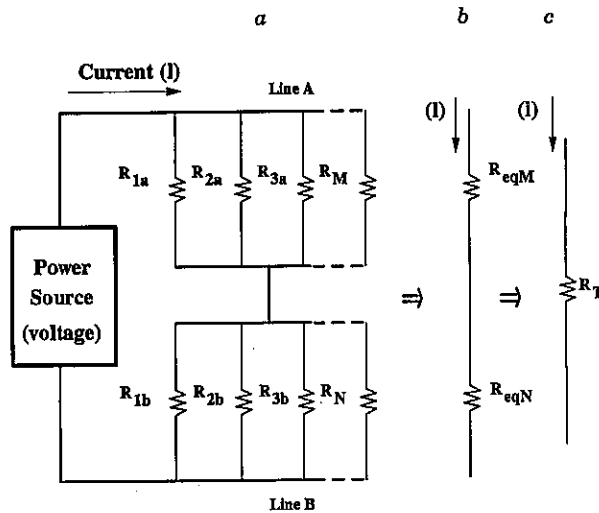


Fig. 4. Diagrams showing the analysis sequence to simplify the electrical circuits for an electrofishing system: (a) Generic circuit for any two-terminal electrofishing system. (b) Simplified circuit showing the parallel resistors attached to each line replaced by their equivalent resistances ( $R_{eqM}$  and  $R_{eqN}$ ). (c) Final circuit is reduced to a single value of resistance ( $R_T$ ).

between the "M" and "N" electrodes) is provided by the water; it is not a "metal-wired" connection. A complete circuit analysis is possible for any electrode array if the individual electrode resistances are known.

Although the generic circuit appears complex, the analysis is readily initiated by calculating the equivalent resistance associated with each terminal (line A or line B) of the power source. Those electrodes attached to a given terminal are actually connected in parallel, and an equivalent resistance can be calculated for each (Brand 1979). These equivalent resistances ( $R_{eqM}$  and  $R_{eqN}$ ) are depicted in Fig. 4b where

$$R_{eqM} = \frac{1}{(1/R_{1a} + 1/R_{2a} + 1/R_{3a} + \dots + 1/R_M)} \text{ ohms} \quad (4)$$

and

$$R_{eqN} = \frac{1}{(1/R_{1b} + 1/R_{2b} + 1/R_{3b} + \dots + 1/R_N)} \text{ ohms.} \quad (5)$$

In equations 4 and 5, the individual electrodes are represented by their corresponding resistance value.

The circuit has now been reduced to a series connection of two resistors:  $R_{eqM}$  and  $R_{eqN}$  (Fig. 4b). The total resistance ( $R_T$ ) for the system (Fig. 4c) is calculated by

$$R_T = R_{eqM} + R_{eqN}. \quad (6)$$

Regardless of the number of electrodes, this analysis technique reduces any single-phase electrofishing system to one equivalent resistance ( $R_T$ ). Although more complicated, the same general techniques can be applied for electrofishing equipment designed with multiple power sources (Harris 1955).

### Resistance Analysis

A resistance analysis is now demonstrated for a hypothetical electrofishing system by using the electrode resistances presented in Fig. 3 for cylinders. Consider a system designed with four cylindrical electrodes that are separated by a sufficient distance to prevent mutual coupling between the electric fields. Three electrodes are attached to line A of the power source, and a single electrode is connected to line B. Two of the cylinders on line A are 1.27 cm in diameter and measure 116 ohms for an immersion depth of 60 cm. The third cylinder on line A is 2.54 cm in diameter and immersed to a depth of 30 cm; its resistance is about 169 ohms. The single cylinder on line B is 60 cm long and 5.08 cm in diameter and has a resistance of 81 ohms. These resistances are for a water conductivity of 100  $\mu\text{S}/\text{cm}$ , but the system is to operate in water of 500  $\mu\text{S}/\text{cm}$ . Therefore, it is necessary to correct the resistance values for the three sizes of electrodes by the conversion ratio of  $c_1/c_2 = 100/500 = 0.2$  (equation 3). The corrected resistance values are about 23, 34, and 16 ohms (Fig. 5a). Figure 5b indicates how the three parallel electrodes connected to line A combine for an equivalent resistance of 8.6 ohms, while the resistance of the single electrode on line B remains unchanged at 16 ohms. The resistance analysis is completed by calculating the total circuit resistance of 24.6 ohms (Fig. 5c).

### Voltage and Current Analysis

It is possible to extend the results from the resistance analysis and to calculate how the system's applied voltage ( $V_s$ ) is proportioned between the two electrode voltages:  $V_A$  and  $V_B$  in Fig. 5. Each electrode's voltage is equal to the ratio of the equivalent resistance for the parallel electrodes ( $R_{eqM}$  or  $R_{eqN}$ ) to the total resistance ( $R_T$ ) times the applied voltage ( $V_s$ ). That is,

$$V_A = \frac{R_{eqM}}{R_T} \times V_s = (8.6/24.6) \times V_s = 0.35 V_s \quad (7)$$

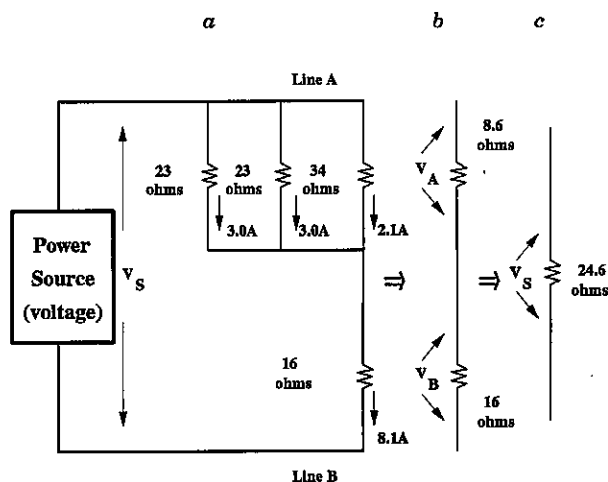


Fig. 5. Progression of a circuit analysis for an electrofishing system having three electrodes on line A and one electrode on line B: (a) Complete electrical circuit with resistance values shown for each electrode. (b) Circuit with the three electrodes on line A replaced by a single equivalent resistance (8.6 ohms). (c) Single value of resistance (24.6 ohms) calculated for the electrofishing system.

and

$$V_B = \frac{(R_{eqN} / R_T) \times V_S}{(16 / 24.6) \times V_S} = 0.65 V_S. \quad (8)$$

Therefore, the three electrodes connected to line A will each receive 35% of the applied voltage (paralleled electrodes always have the same applied voltage even if their resistance values are different), while the single electrode on line B will dissipate 65%. Note that the sum of the two electrode voltages must always equal the applied voltage. That is,

$$V_S = V_A + V_B. \quad (9)$$

To continue this analysis, assume that the power supply is adjusted to an applied voltage of 200 volts. The electrode voltages  $V_A$  and  $V_B$  are calculated by equations 7 and 8 to be 70 and 130 volts, respectively. All of the voltages and resistances for the four-electrode system are now determined, and Ohm's Law ( $I = V/R$ ) can be applied to calculate the current conducted by each electrode (Fig. 5) or the total current conducted by the system (200 volts / 24.6 ohms = 8.1 amps).

### Power Analysis

The circuit analysis is completed by calculating the electrical power dissipated in the electric fields

surrounding each of the four electrodes. Three expressions for power are available, and the most convenient can be chosen:

$$\text{Power} = VI = V^2/R = I^2R \text{ watts.} \quad (10)$$

For this example, the wattages are 210 W (3.0 amps  $\times$  70 volts) dissipated around each of the 1.27-cm cylinders, 147 W (2.1 amps  $\times$  70 volts) for the 2.54-cm electrode, and 1,053 W (8.1 amps  $\times$  130 volts) for the single 5.08-cm electrode. The total power delivered into the water is 1,620 W. These wattage values are valid only for water conductivity of 500  $\mu\text{S}/\text{cm}$ .

### Comments on Power Supply Instrumentation

Electrofishing equipment is usually instrumented to measure some combination of voltage, current, and power at the generator or equipment control panel. For the preceding example, the voltmeter, ammeter, and wattmeter at the generator would read 200 volts, 8.1 amps, and 1,620 watts. However, the individual electrode voltages, currents, or power (as calculated in the example) could not be determined with this metering without knowing the resistance values for the electrodes. It is unsettling to realize that the metering on electrofishing equipment is basically a monitor of the power supply, and that this metering does not provide comparative information regarding the electric fields generated in the water. The on-board metering serves as a placebo for the equipment operators. Equipment operators should never expect two electrofishing units that are connected to dissimilar electrode arrays to function alike just because the voltage, current, or power meters read the same. Consistent operational procedures and equipment standardization can only be developed based on comparative in-water measurements with known electrode configurations.

### Voltage Measurements in a Volume of Water

The engineering approach to electrical field theory involves complex equations and electrical parameters that are often difficult for the fishery biologist to apply. Most field practitioners would prefer to forego these mathematical complexities; they simply desire comparative information for an educated selection of an electrode system. For electrofishing applications, it is fortunate that any

electric field is adequately defined by the distribution of the voltage in the water, and these voltages are not difficult to measure and plot on a graph. To better understand the mechanism by which voltage patterns are created in the water, it is enlightening to present a quasi-technical discussion that illustrates the significance of the metal-to-water interface in the creation of any three-dimensional electric field.

### *Quasi-technical Concepts for Electric Fields in Water*

All electrofishing arrays have two similarities: the electrodes are constructed with high conductivity metals, and the water surrounding the electrodes exhibits a much lower electrical conductivity than the metal. This difference in conductivity (conductivity of metals is typically  $10^{12}$ , whereas that of fresh water is about  $10^3 \mu\text{S/cm}$ ) necessarily describes an electrical circuit having most of its resistance associated with the water; the conductivity of the metal is simply too high to contribute a significant resistance compared with the water. Additionally, the water is a homogeneous material; the electrical characteristics of the water near the electrode are the same as the water at some distance from the electrode. These facts imply that, somehow, the geometry at the metal-to-water interface (or interfaces in the case of multiple electrodes) must be responsible for the creation of electric fields having different spatial characteristics.

It is instructive to consider a long, smooth-metal cylinder and to imagine the volume of water surrounding this electrode as being divided into a large number of identical cubes. Since the water is homogeneous, each cube exhibits the same electrical resistance; there is nothing uniquely different about any particular cube of water. This mental process converts the volume of water into a network of equally valued resistors, and we can now speculate how the electrical currents must conduct through this maze of resistors and generate an electric field.

Due to its high electrical conductivity, the entire length of the metal cylinder is considered energized to the same potential of voltage; there is no difference in voltage along its length. The energy loss within the cylinder may then be assumed negligible, and each incremental length of the cylinder is electrically identical to the next. These assumptions allow us to examine a single, incremental cross section of the cylinder and to direct attention to the flow of the electrical current at the metal-to-

water interface. Figure 6a shows a cross-sectional view of an incremental length of the cylinder with the cubes of water aligned around the cylinder in concentric rings. Note that the coaxial (circular) symmetry of the cubes precludes any current flow in a circumferential direction; all the current moves in a radial direction away from the cylinder. Each cube of water may now be replaced by its symbol for electrical resistance to give an indication of the in-water wiring (Fig. 6b).

In studying Fig. 6, note that the electrode's surface area limits the number of cubes that may actually have a direct metal contact. However, as the distance from the electrode is increased, a greater number of cubes enter into the electrical circuit. Observe how the cubes in a particular

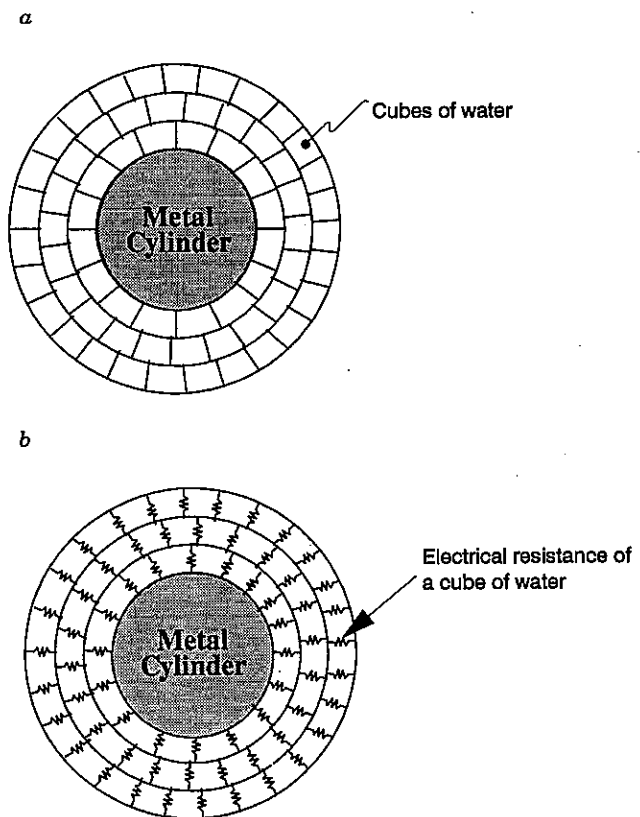


Fig. 6. Diagrams illustrating the metal-to-water interface for a cylindrical electrode: (a) Cross section of the electrode surrounded by squares that represent the circular alignment of cubes of water around the electrode. (b) Electrical resistors are substituted for the individual cubes of water to create a visualization of the in-water electrical circuit.

concentric ring act as a group of parallel resistors, and these successive groups become effectively wired in series as the electrical charge moves radially from one concentric ring to the next. Therefore, the circuit diagram for this axial segment of the cylindrical electrode can be reduced to a series circuit (Fig. 7), where  $R_1, R_2, R_3 \dots R_N$  represent the equivalent resistances of the first, second, third...Nth group of concentric (parallel) resistors.

As the radii of the concentric rings increase, the number of cubes per concentric ring also increases. In this manner, the effective resistance for each consecutive ring decreases as more parallel resistors are added; that is,  $R_1 > R_2 > R_3 > \dots > R_N$ . This phenomenon of decreasing resistance implies that the incremental voltages generated across the successive concentric rings must decrease in some nonlinear manner as the distance away from the surface of the electrode is increased. Furthermore, it is the shape and size of an electrode that determines how the cubes initially become "inter-wired" into the water to generate a unique electric field pattern.

This conceptualization of concentric rings surrounding the cylindrical electrode provides a mental image of what is meant by the term voltage gradient; voltage gradient is the in-water voltage that exists across an individual concentric ring. The first concentric ring always has the greatest incremental resistance ( $R_1$ ) and must, therefore, exhibit the largest voltage gradient. When comparing electrodes of different size, it is helpful to consider that larger-surfaced electrodes expose more metal to the water, and this exposure decreases the initial resistance value of  $R_1$ . Any reduction in the initial resistance means that less voltage is dissipated near the electrode. It becomes a matter of algebra. If voltage is not dissipated close to an electrode, it becomes available at distances away from the electrode. Thus, larger-surfaced electrodes inherently extend their electric fields a greater distance by reducing the voltage gradient near the electrodes, and smaller

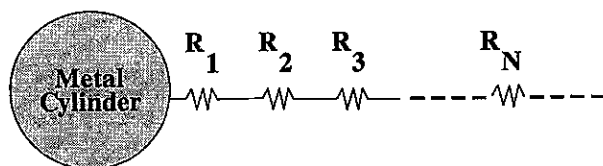


Fig. 7. Equivalent series circuit for a cylindrical electrode.

electrodes collapse their fields by increasing the voltage gradients near the electrodes. The above discussion is based on a circular geometry, but the reader can readily expand the basic tenets to any electrode configuration. With these mental perceptions, equipment operators can develop intuitive guidelines for modifying electrodes to particular field applications.

### *In-water Voltage Measurement Techniques*

I present two empirical methods for determining the distribution of voltages in water. One method measures the in-water voltage as a function of distance, and the second method measures the incremental voltages (voltage gradients) at discrete locations in a volume of water. The first method develops a voltage versus distance profile with the same instrumentation described for measuring the resistance of electrodes. The second method requires a special probe that connects to a voltmeter or cathode ray oscilloscope and directly measures voltage gradient. Voltage gradient can also be converted to a power density measurement with the equation

$$D = cE^2 \quad (11)$$

where,

- D = power density ( $\mu\text{W}/\text{cm}^2$ ),
- c = conductivity of the water ( $\mu\text{S}/\text{cm}$ ), and
- E = voltage gradient ( $\text{V}/\text{cm}$ ; Kolz 1989).

At present, there are no instruments marketed that directly measure power density, but I predict that power density information will eventually prove valuable in providing electrofishing threshold data for comparing various species of fish.

### **Method 1: Voltage Profiles**

It is convenient to describe what is meant by a voltage profile through illustration. Figure 8 shows an experimental setup having two identical electrodes (A and B) immersed in water to some convenient depth (D) and separated by a distance (X). The electrodes are driven by an AC power source similar to that depicted in Fig. 2. One test lead of the voltmeter has a direct wire connection to the "A" electrode, and the second lead is fitted with an extended length of insulated wire (about #20 gauge) that has the end of its conductor exposed for approximately 2 mm. With this apparatus, the voltmeter can measure the electrical potential between the "A" electrode and the tip of the

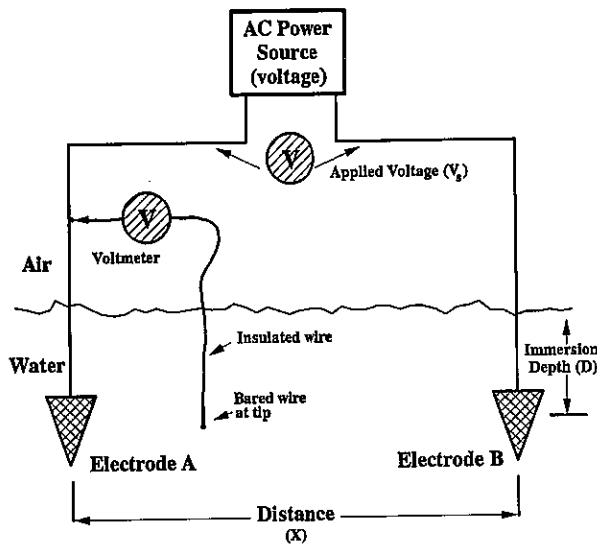


Fig. 8. Circuit configuration and metering for measuring voltage profiles.

wire probe as the probe is moved throughout the volume of water.

A voltage profile is produced by plotting the voltmeter readings as a function of the probe's location. For example, the probe might be moved through the water along a transect between the centroids of the two electrodes; along this particular path, the voltage readings at three locations are predictable. With the probe at zero distance (i.e., touching the "A" electrode), the voltage reading is zero; both voltmeter leads are electrically connected to the same piece of metal. When the probe is midway between the two electrodes, the geometric symmetry of the apparatus requires the voltage reading to be one-half the applied voltage (50% of  $V_s$ ). And finally, when the probe makes contact with the "B" electrode, the meter will read the applied voltage ( $V_s$ ). The interspatial readings between these predicted values can also be measured with the voltmeter, and Fig. 9 shows a generalized voltage profile for the two identical electrodes.

The S-shaped voltage curve depicted in Fig. 9 results from the decreasing values of effective in-water resistance as described in the quasi-technical discussion. The S-curve can be interpreted as showing that one-half the supply voltage and one-half of the available power are dissipated in the volume of water surrounding each of the electrodes. In fact, electrofishing systems operating with two identical electrodes are often described as being a "balanced" electrode array. This conclusion

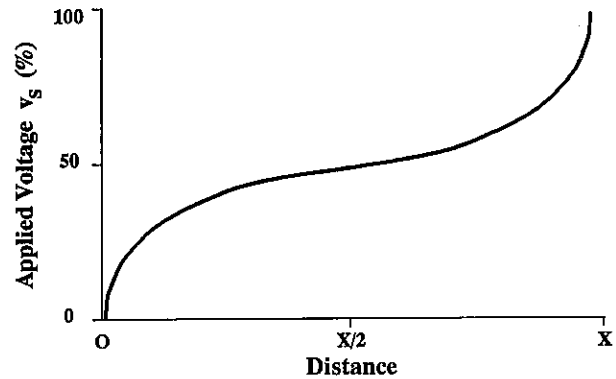


Fig. 9. Generalized voltage profile for two identical electrodes.

is substantiated by applying the analysis techniques previously described and noting that any balanced electrode system implies that  $R_{eqM} = R_{eqN}$ ; similar electrodes must have equal resistances (Fig. 4). Furthermore, the relative curvatures along each end of the S-curve reflect a reversed geometric symmetry, and the two halves of the S appear balanced.

Voltage profiles can also be measured for electrode arrays that are dissimilar or unbalanced. Dissimilar electrodes simply displace and alter the shape of the S-profile, and the two halves of the S-curve will no longer display the same relative curvatures or the same percentages in applied voltage. The voltage profiles can be used to graphically demonstrate spatial differences between the electric fields generated by various electrode configurations. In fact, an electrode design can purposely be chosen to dissipate more voltage or power at one particular electrode. For example, backpack electrofishing equipment can be designed to direct more power into the hand-held electrode for capturing fish than into the trailing electrode.

A voltage profile can be developed into a voltage gradient profile by noting that voltage gradient is defined by the derivative of the voltage profile ( $E = dV/dx$ ). In words, the slope of the tangential line at any point on the voltage profile is the value of the voltage gradient at that location. The S-shape of the voltage profile will always produce a voltage gradient profile having a U-shaped curve (Fig. 10). The two arms of the U will be symmetric or non-symmetric depending on whether the system is balanced or unbalanced. The shape of the U-curve is highly significant in electrode design. If the U rises sharply and bottoms quickly, the electrode

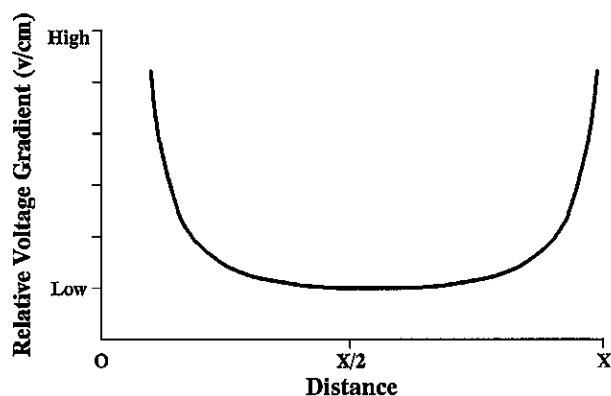


Fig. 10. Generalized voltage gradient profile for two identical electrodes.

design will develop high voltage gradients close to the surface of the electrode and will electrify only a small volume of water. In contrast, a U-curve that decays more slowly will produce significant levels of voltage gradient at distances farther from the electrode and thereby extend the effective electrofishing range. Voltage gradient profiles obviously provide another means for comparing the electric fields generated by different electrodes.

Neither the voltage nor voltage gradient profiles change significantly with the values in water conductivities normally encountered when electrofishing. Nearly identical profiles will result for a given array regardless of whether the electrodes are measured in low conductivity ( $50 \mu\text{S}/\text{cm}$ ) or high conductivity ( $5,000 \mu\text{S}/\text{cm}$ ) water, provided that the applied voltage is kept constant on the electrodes. Therefore, it is necessary to record only one voltage profile for an electrode, and these data are then transferable to any water condition. However, the amount of power dissipated by the electrodes is directly proportional to the conductivity of the water; doubling the water conductivity doubles the power and vice versa. Voltage profiles are almost independent of water conductivity and power dissipation, which verifies that voltage measurements cannot be used to standardize electrofishing operations.

The voltage profiles and voltage gradient profiles can be measured at any convenient electrode voltage ( $V_s$ ). Both types of profiles can be linearly scaled to other operating voltages. For example, if the profiles were measured at 100 volts, the ordinate values of the profiles could then be scaled by a factor of 4 when operating the system at 400 volts.

## Method 2: Direct Voltage Gradient Measurements

It is possible to make direct in-water measurements of voltage gradient by connecting a special probe to either a cathode ray oscilloscope (CRO) or digital voltmeter (DVM). This instrumentation is probably more complex and expensive than the voltmeter previously described, but it has the advantage of being able to make on-site readings for timely equipment adjustments.

The voltage gradient probe (Fig. 11) consists of a pair of insulated wires attached at one end to the input terminals of a CRO or DVM and mechanically supported on the other end by an electrically insulated rod. The rod serves as a handle for the probe, and its length is determined by the depth of the water being measured. The pair of wires extends past the end of the rod, and each wire is stripped of its insulation to expose a length of about 2 mm of bare wire with a diameter of about 1 mm. When immersed into an electrical field, this probe allows the differential voltage existing between the two bared wires to be measured with the CRO or DVM. It is convenient to separate the bared wires by 1 cm and thereby measure voltage gradient directly in volts per centimeter.

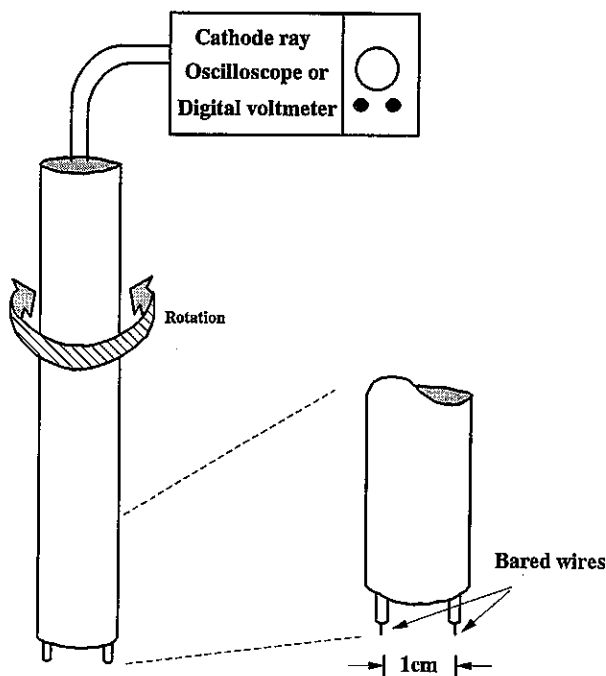


Fig. 11. Diagram showing the configuration of a voltage gradient probe.

The voltage gradient probe is usually inserted into the electric field at a near-vertical angle to the surface of the water. When positioned in the water, the probe must be rotated for a maximum reading because voltage gradient is a vector (directional) quantity (Rogers 1954). The CRO or DVM will indicate two maxima and two nulls with each rotation of the probe. By probing a volume of electrified water at known depths, the gradient readings at each depth may be plotted to create a family of voltage gradient maps (analogous to a geographic contour map) for a three-dimensional analysis. It is often convenient to have predetermined those thresholds of voltage gradient having biological importance (electrotaxis, stun, tetany, etc.) and to just locate these constant gradient loci in the water. Explicit voltage gradient maps are not always necessary for comparing electrode arrays.

## Test Procedures

The empirical data compiled for this study used only voltage profiles (method 1); the voltage gradient probe (method 2) was not applied as a measurement tool. Voltage profiles were recorded for 18 balanced electrode configurations.

### *Description of the Test Electrodes*

Five basic electrode configurations were selected as representative of the geometric shapes common to electrofishing applications: spheres, cylinders, circular loops, Wisconsin arrays, and vertical plates.

**Spheres.** Two sizes of spheres, 15.2 and 27.7 cm diameter, were measured at immersion depths of 30 and 40 cm, respectively.

**Cylinders.** The voltage profiles for four sizes of cylinders, with diameters of 0.64, 1.27, 2.54, and 5.08 cm, were recorded. All cylinders were immersed vertically from the water's surface to a depth of 60 cm.

**Loops.** Two horizontal loops were suspended in the water at a depth of 30 cm. The smaller loop measured 36 cm in diameter and was constructed with 0.64-cm-diameter tubing. The larger loop was 61 cm in diameter and was constructed with 1.27-cm-diameter tubing.

**Wisconsin arrays.** A common electrofishing array consists of vertical cylinders (often called rods or droppers) suspended into the water from a supporting circular ring that is attached to a

boom above the water. This electrode configuration became popular following its description by Novotny and Priegel (1974) and is commonly known as the Wisconsin array. Seven variations of this array were tested. Four of the arrays were constructed by using a 30.5-cm-diameter ring to support four or six 60-cm-long cylinders with diameters of 0.64 or 2.54 cm. The cylinders were spaced equidistantly around the circumference of the supporting ring. The other three arrays were constructed similarly except that a 58-cm ring provided the support for 4 or 6 droppers, and the cylinder diameters were 0.64 or 2.54 cm.

**Vertical plates.** Flat aluminum plates measuring 0.32 cm thick by 122 cm wide were immersed vertically into the water to depths of 15.2, 30.5, and 45.7 cm.

### *Measurement Site and Techniques*

The electrode measurements were conducted at the Hydraulics Research Laboratory of the Bureau of Reclamation in Denver, Colorado. This facility has numerous 3-m-wide indoor canals constructed with concrete walls and floors. The minimum water depth was 1.4 m, and the canals were fully accessible from above through a grid of metal grates. The water conductivity varied from 111 to 190  $\mu\text{S}/\text{cm}$ . The voltage data were recorded only during those periods when the canals were not in major use by other researchers; the surface of the water was usually almost mirror-perfect. Each pair of test electrodes was powered by a voltage-adjustable autotransformer operating from a standard 60-Hz AC main. The applied voltage was consistently set to 100 volts so that each balanced electrode dissipated 50 volts. For added safety and the elimination of possible leakage currents, the autotransformer was connected to the mains through an isolation transformer. The section of canal in which the electrodes were measured was found to be free of any metal structures that might create a shock hazard or distort the electric field.

For recording the voltage profiles, a wooden beam was fitted with a centimeter scale for measuring distance and suspended above the center of the canal between the test electrodes. A bracket was constructed to slide along this beam and support the "bared" voltmeter lead that was weighted vertically into the water. In this manner, the end of the wire extending into the water could be adjusted to any desired depth, and the slider was

simply moved horizontally along the beam while recording the voltmeter and distance readings.

The voltage profiles for the cylinders were measured at a separation of 2.7 m. This distance was increased to 4 m for the spheres, loops, Wisconsin arrays, and vertical plates. The effect of close electrode spacing is to possibly cause the middle portion of the S-curve to display an exaggerated slope because mutual coupling may exist between the two electric fields. The middle of the S-curve should display a minimal slope when the two electrodes are not interacting. In retrospect, it would have been better to measure all of the electrodes with a separation of 4 m, but this inconsistency is not judged detrimental in the following experimental results.

## Presentation of In-water Electrode Measurements

Data are presented for 18 electrode configurations in a generalized format that can apply to a variety of electrofishing requirements. The following includes a table listing the empirical resistance values, a table comparing the spatial electric fields generated by each type of electrode, a set of voltage profiles, a graphic summary displaying calculations of voltage gradient and the squared values of voltage gradients, and a discussion regarding the voltage gradient vector.

### Values of Electrode Resistance

The calculated resistance values for the 18 electrode configurations are presented in Table 1. Adequate spatial separation was provided between the electrodes to ensure minimal coupling between the electric fields; therefore, the resistance values are representative of a single, isolated electrode. All values of electrode resistance have been normalized for water having an electrical conductivity of 100  $\mu\text{S}/\text{cm}$ , but these resistances can readily be converted for actual field applications to any value of water conductivity by applying equation 3. The resistances presented in Table 1 and Fig. 3 are directly applicable to any electrofishing system using these particular electrode configurations.

Boat hulls are often wired as cathodes when electrofishing with direct current or pulsed direct current, and it would have been desirable to present resistance measurements for various sizes of hulls in this report. However, the dimensions of the

indoor test facility precluded this opportunity. Certainly, boat hulls can be measured by the procedures already described, but the awkward logistics of having to interwire between two boats (each boat being an electrode) may be avoided by considering the following interactive solution. First, determine the electrical resistance of the anodes by the procedures already described. The metal-to-water interface of a boat hull is large in comparison to that of the anodes, so most of the electrode resistance is associated with the anodes. Approximate electrical calculations may be performed by assuming that the hull's resistance is one-tenth that of the anode resistance. Based on these initial calculations, the equipment may be operated and the estimated value of the hull resistance corrected by using the actual voltage and current readings displayed at the control panel.

Table 1. *Electrical resistance of various electrode configurations.<sup>a</sup>*

Electrode configuration <sup>b</sup>	Electrical resistance (ohms) <sup>c</sup>
Spheres	
15.2 cm	89
27.7 cm	55
Cylinders (60-cm length)	
0.64 cm	142
1.27 cm	117
2.54 cm	99
5.08 cm	81
Horizontal loops	
0.64 $\times$ 36 cm	86
1.27 $\times$ 61 cm	46
Wisconsin array (60-cm rods, 30.5-cm ring)	
four rods at 0.64 cm	57
six rods at 0.64 cm	50
four rods at 2.54 cm	46
six rods at 2.54 cm	43
Wisconsin array (60-cm rods, 58-cm ring)	
four rods at 0.64 cm	45
four rods at 2.54 cm	37
six rods at 2.54 cm	31
Vertical plates (0.32 cm thick $\times$ 122 cm wide)	
15.2 cm immersion	54
30.5 cm immersion	39
45.7 cm immersion	30

<sup>a</sup> All electrodes constructed with aluminum materials.

<sup>b</sup> Measurements are for diameters unless stated otherwise.

<sup>c</sup> Single electrode in 100- $\mu\text{S}/\text{cm}$  water.



### *Spatial Comparisons of Electric Fields*

A voltage profile was recorded for each of the 18 pairs of electrodes on a transect intercepting their vertical centroids. For example, the voltage profiles for spheres were measured along a line connecting through their centers. It was actually only necessary to measure half of the S-curve for each pair of electrodes because the electrical loads were balanced and exhibited the reversed geometric symmetry described previously.

The voltage profiles indicate how effectively an electrode projects energy into the water. For example, if the S-curve exhibits an abrupt curvature and rapid dissipation of voltage in proximity to an electrode, the resultant electric field will be spatially limited to a small volume. Conversely, larger electric fields are generated by electrodes that exhibit more linear (less bent) S-curves. Thus, voltage profiles offer a basis for comparing the size of electric fields by correlating these data in some consistent manner.

I chose to analyze the data by interpolating those distances from the voltage profiles at which 50 and 80% of the applied voltage (25 and 40 volts) was dissipated. These two distances provide information regarding the relative curvature of the S-curve; short distances imply abrupt curvatures and vice versa. However, I found these distances awkward to interpret and, therefore, arbitrarily selected the 15.2-cm (6-inch) sphere as a "reference" electrode for comparison. Subsequently, ratios were calculated by dividing the two distances interpolated from the individual voltage profiles by the corresponding distances actually measured for the 15.2-cm sphere: 8.4 cm at 50% voltage and 35.7 cm at 80% voltage. The resulting distance ratios then relate the rate at which the voltage changed for a test electrode compared with that of the reference sphere. This comparison method offers a technique that can be extended to any electrode configuration. Also, this comparison is independent of the magnitude of applied voltage; the technique is based only on the measurement of a distance at a given percentage of applied voltage.

The two distance ratios calculated for each electrode can be directly correlated with the levels of voltage gradient generated in the water. For example, the 50% voltage ratio indicates the relative magnitude of the voltage gradient in proximity to the electrode; a small ratio implies an electrode that dissipates its voltage in a short distance and thereby generates high voltage gradients. In contrast, the ratios calculated for the 80% voltage

provide an index relating to the expanse of the horizontal electric field; a large ratio implies that a significant level of voltage gradient extends a greater distance from an electrode. Table 2 summarizes these two distance ratios for the 18 electrodes and ranks these ratios from the smallest to the largest. This ranking allows the reader to systematically compare the relative magnitudes of voltage gradients and the extent of the horizontal electric field among the 18 electrode configurations.

For the 18 test electrodes, the highest voltage gradient was produced by the 36-cm horizontal loop, while the 45.7-cm vertical plate generated the lowest. As predicted, the same two electrodes also project the shortest and farthest electric fields. Note that all the electrodes tested, with the exception of the vertical plates, display a high degree of radial symmetry. This symmetry implies that these electrodes can be rotated about their vertical axis without significant changes in their voltage profiles. The vertical plates are not radially symmetric, and therefore create asymmetric electric fields that project their farthest on a transect normal to the surface of the plate. The comparative rankings in Table 2 are based upon the optimal voltage profiles for the plates as measured normal to their surface.

Observe that the two rankings in Table 2 are not consistent. This inconsistency is caused by the unusual geometry of Wisconsin arrays. In proximity, the individual droppers of these arrays generate levels of voltage gradients characteristic of individual cylinders. At greater distances, however, the group of droppers mutually interacts to extend the electric field to a greater distance. The shape of the S-curve is therefore significantly altered from those curves generated by electrodes having a single, continuous surface.

### *Voltage Profiles*

The voltage profiles for the 18 electrodes are grouped according to their basic configuration (spheres, cylinders, loops, Wisconsin arrays, and vertical plates) and presented in Figs. 12 through 17. The empirical data for spheres and cylinders were fit to known mathematical expressions (Novotny and Priegel 1974), and statistical correlation coefficients of greater than 0.995 were achieved. There are no mathematical expressions derived from electrical field theory for the loops, Wisconsin arrays, and vertical plates, and I present only the raw data in Figs. 14 through 17. All graphs are presented to the same scaling to allow comparisons among the six groups.

Table 2. Distance ratios and ranking for comparing the relative magnitudes of voltage gradient and the horizontal projections of the electric fields for various electrode configurations when referenced to a 15.2-cm-diameter sphere.

Electrode configuration <sup>a</sup>	Sphere distance ratio and ranking			
	50% voltage		80% voltage	
	Distance	Rank	Distance	Rank
Spheres				
15.2 cm <sup>b</sup>	1.00	5	1.00	4
27.7 cm	1.89	11	1.66	10
Cylinders (60-cm length)				
0.64 cm	0.47	2	0.76	2
1.27 cm	0.83	3	1.00	3
2.54 cm	1.19	7	1.15	5
5.08 cm	1.70	9	1.35	6
Horizontal loops				
0.64 × 36 cm	0.19	1	0.58	1
1.27 × 61 cm	1.15	6	1.42	8
Wisconsin array (60-cm rods, 30.5-cm ring)				
four rods at 0.64 cm	1.27	8	1.49	9
six rods at 0.64 cm	1.81	10	1.70	11
four rods at 2.54 cm	1.94	13	1.82	13
six rods at 2.54 cm	2.63	15	2.21	16
Wisconsin array (60-cm rods, 58-cm ring)				
four rods at 0.64 cm	0.99	4	1.42	7
four rods at 2.54 cm	1.89	12	1.81	12
six rods at 2.54 cm	2.60	14	2.11	14
Vertical plates <sup>c</sup> (0.32 cm thick × 122 cm wide)				
15.2 cm immersion	3.18	16	2.19	15
30.5 cm immersion	4.52	17	2.82	17
45.7 cm immersion	5.73	18	3.23	18

<sup>a</sup>Measurements are for diameters unless stated otherwise.

<sup>b</sup>The voltage profile of the reference sphere measured 8.4 cm at 50% voltage and 35.7 cm at 80% voltage.

<sup>c</sup>The voltage profiles for the vertical plates were measured along transects normal to their surface.

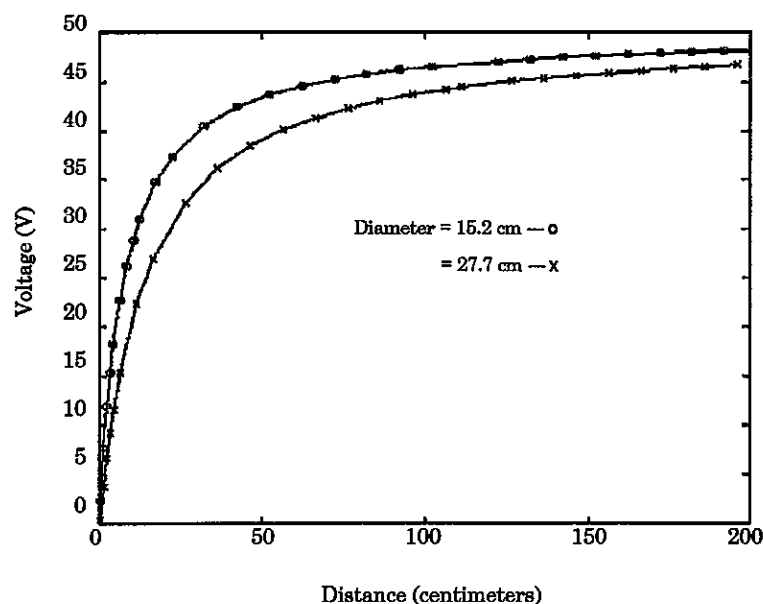


Fig. 12. Voltage profiles for two spheres having diameters of 15.2 and 27.7 cm.

Fig. 13. Voltage profiles for four cylinders.

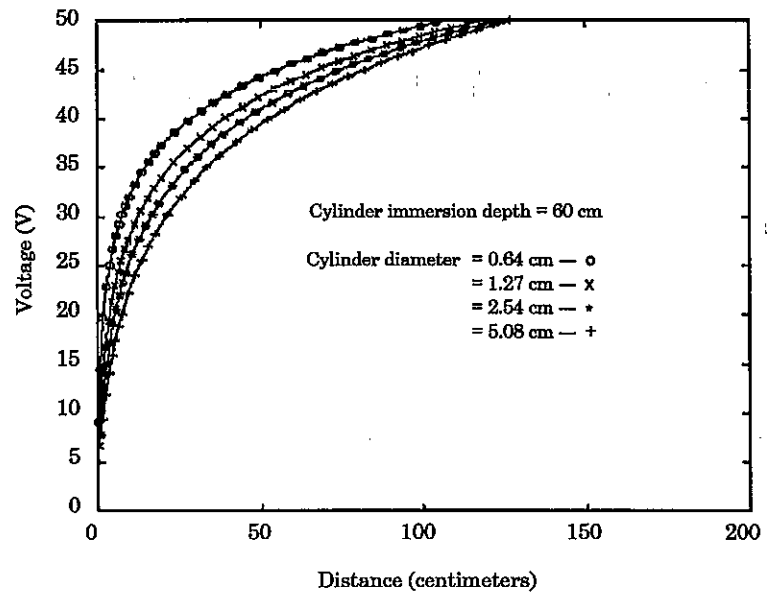
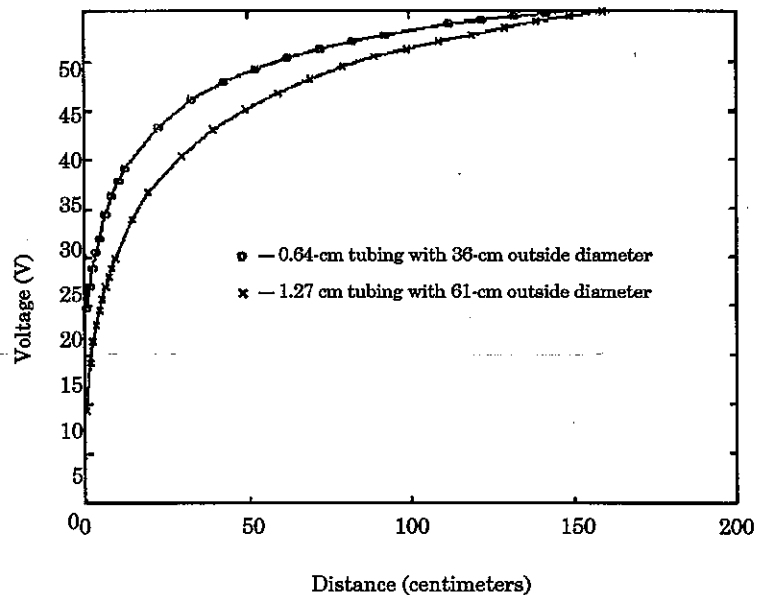


Fig. 14. Voltage profiles for two horizontal loops.



### *Voltage Gradient Profiles*

The mathematical derivatives of the voltage profile curves were derived using standard numerical techniques (De Boor 1978) to calculate the voltage gradient profiles shown in Figs. 18 through 23. Each figure displays two voltage gradient curves that correspond to the six electrode groups described previously. For example, Fig. 13 is used to develop the voltage gradient profiles of Fig. 19 for

cylinders having diameters of 0.64 and 5.08 cm. The voltage gradient profiles for the cylinders having diameters of 1.27 and 2.54 cm could also be added to Fig. 19, but to simplify the graphics only the two profiles that represent the extremes for a given group are presented. The gradient profiles for those electrodes not shown would obviously fit somewhere between.

Except for the spheres and cylinders, for which data were correlated with mathematical expres-

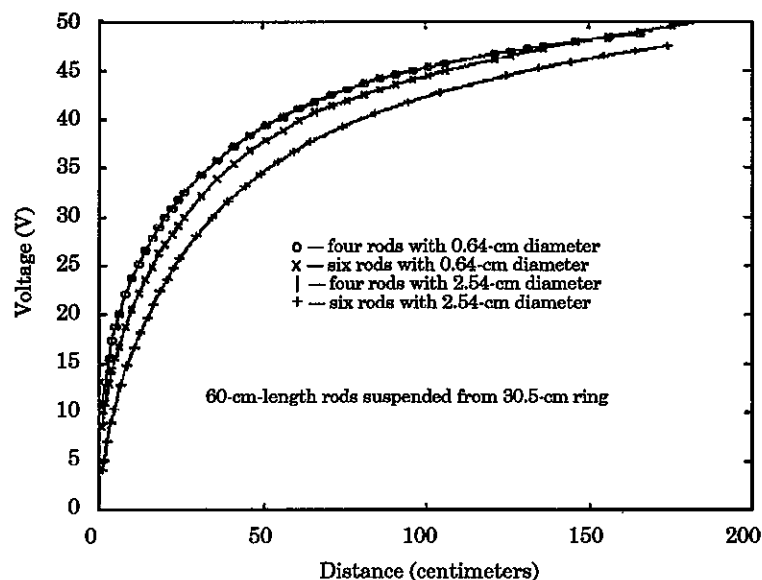


**Fig. 15.** Voltage profiles for Wisconsin arrays with four and six rods suspended from a 30.5-cm supporting ring.

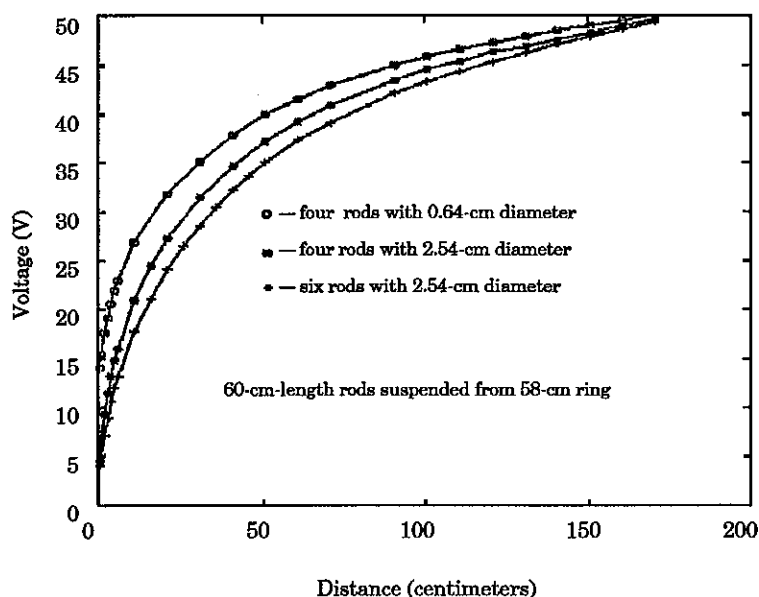


**Fig. 16.** Voltage profiles for Wisconsin arrays with four and six rods suspended from a 58-cm supporting ring.

sions, the voltage gradient profiles have a wavy appearance caused by measurement artifacts. The numerical calculations for voltage gradient proved to be extremely sensitive to incremental variations in the slope of the voltage profiles, and I found that a measurement error as small as 0.1 volt could create a noticeable undulation in a voltage gradient curve. I will leave it to the reader to mentally average a smooth curve through these experimentally induced oscillations.

The initial values of voltage gradient plotted on Figs. 18 through 23 are not to be interpreted as the maximum values of voltage gradient generated in proximity to an electrode. It would require a refined measuring technique to extrapolate this maximum from a voltage profile, and this level of sophistication was beyond the intent of the study. Furthermore, it should be a standard practice when electrofishing to protect the fish from entering this region of the electric field. The most haz-

Fig. 17. Voltage profiles for three vertical plates measured along a transect normal to their surface.

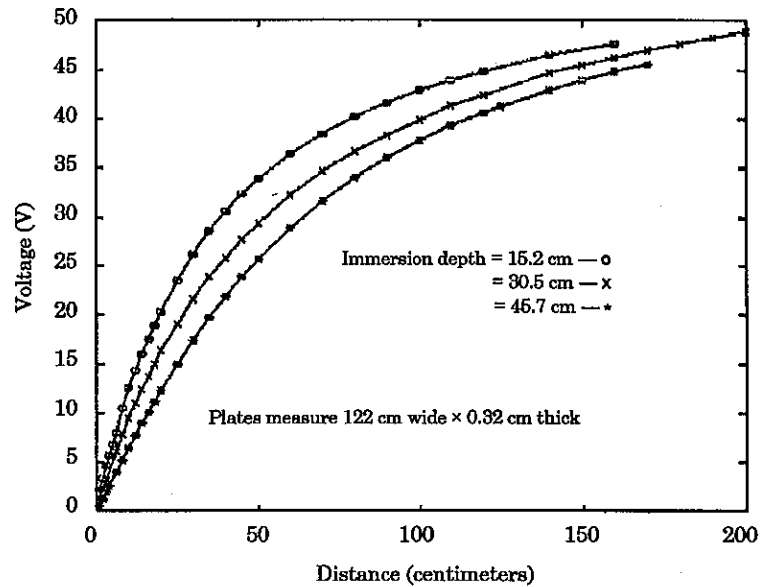
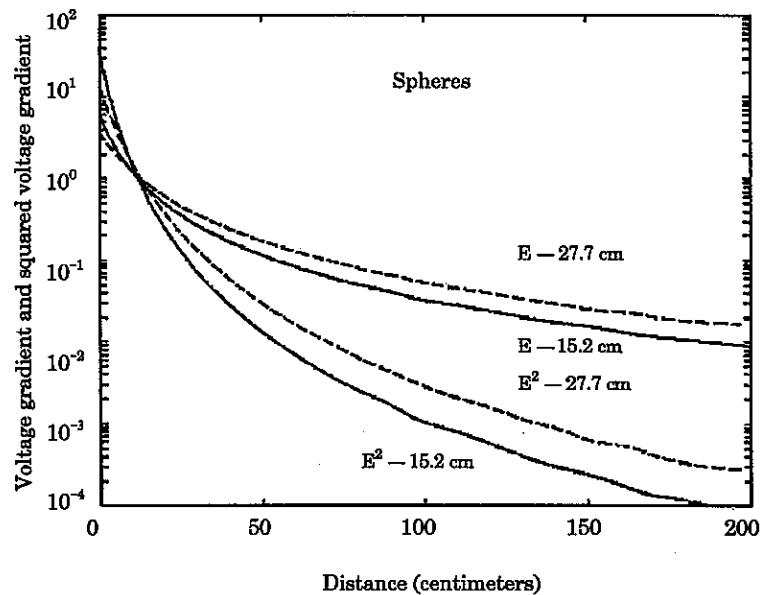


Fig. 18. Profiles of voltage gradient ( $E$ ) and the squared value of voltage gradient ( $E^2$ ) for two spheres having diameters of 15.2 and 27.7 cm.



ardous position for fish in an electric field is always next to the electrodes, and the fish should not be allowed to touch the electrodes.

Figures 18 through 23 show two additional curves that are calculated by taking the square of each value for voltage gradient ( $E^2$ ). These curves are provided to emphasize that power density is actually proportional to  $E^2$  (equation 11), and the steep slope of these  $E^2$  curves demonstrates how quickly power density diminishes with distance.

### Discussion of the Voltage Gradient Vector

Voltage gradient is defined as a vector quantity that has magnitude and direction (Rogers 1954). However, the voltage gradient profiles shown in Figs. 18 through 23 were developed without emphasizing any vector relation for the gradient; only the magnitudes of the gradient are presented. For these figures, two of the three directional components are justifiably ignored be-

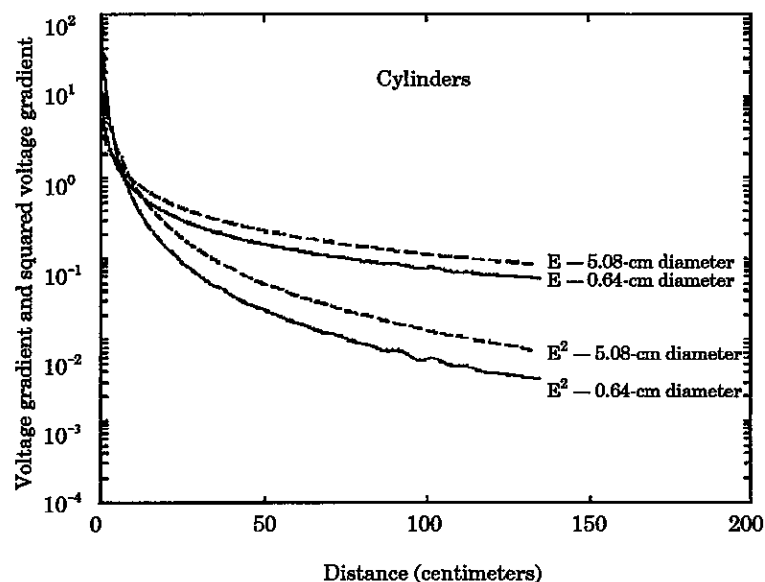


Fig. 19. Profiles of voltage gradient ( $E$ ) and the squared value of voltage gradient ( $E^2$ ) for two cylinders having diameters of 0.64 and 5.08 cm.

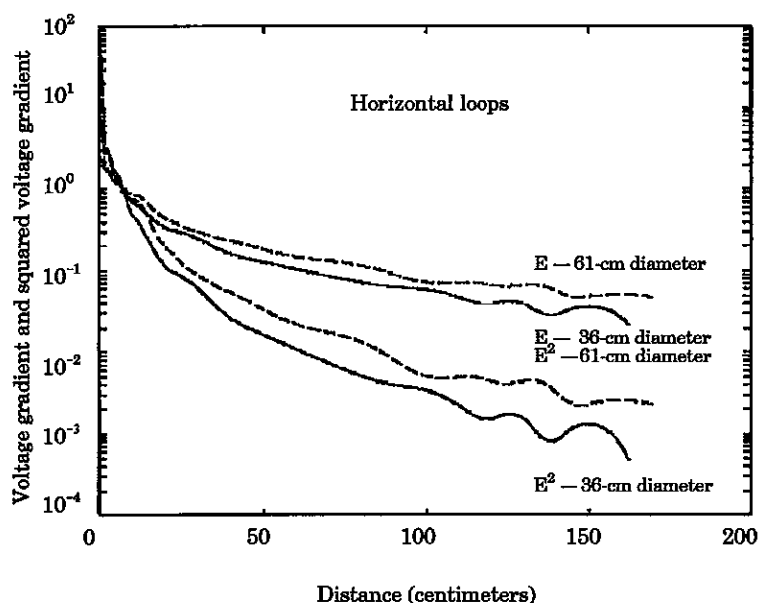
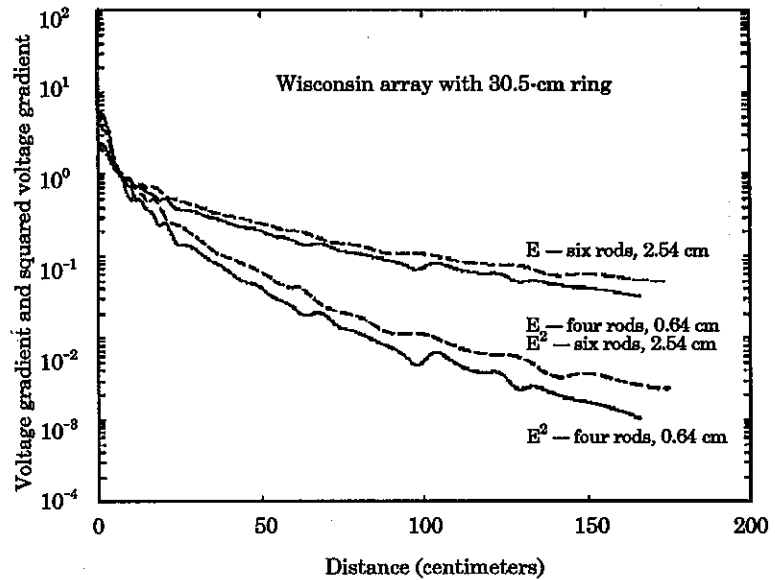


Fig. 20. Profiles of voltage gradient ( $E$ ) and the squared value of voltage gradient ( $E^2$ ) for two horizontal loops having diameters of 36 and 61 cm.

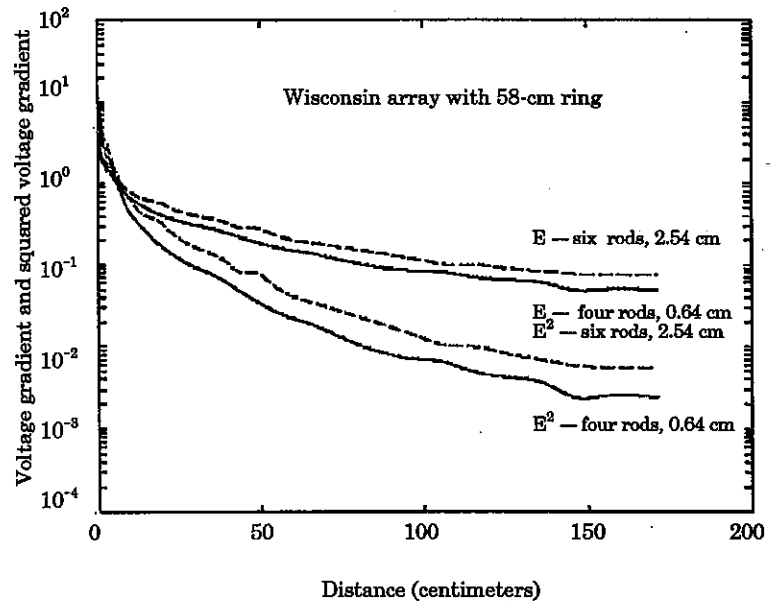
caused the voltage profiles were purposely recorded along a transect intercepting both the vertical and horizontal centroids of the electrodes. The geometric symmetry of this particular transect ensures that the vertical and lateral components of the voltage gradient are zero (or at least minimized). Therefore, the voltage gradient profiles illustrated in Figs. 18 through 23 are actually calculations of the magnitude of the radial component of voltage gradient in the horizontal plane.

The profile techniques can, however, be extended to provide information for all three components of voltage gradient: radial, lateral, and vertical. For information regarding the vertical voltage gradient, the measurement involves recording several profiles at different depths in the same vertical plane and then noting the voltage differences between the profiles. The same procedure applies for the lateral components of voltage gradient, except that the data are recorded along

**Fig. 21.** Profiles of voltage gradient ( $E$ ) and the squared value of voltage gradient ( $E^2$ ) for Wisconsin arrays with four and six rods suspended from a 30.5-cm supporting ring.



**Fig. 22.** Profiles of voltage gradient ( $E$ ) and the squared value of voltage gradient ( $E^2$ ) for Wisconsin arrays with four and six rods suspended from a 58-cm supporting ring.



several radial transects in a common horizontal plane. Figure 24 illustrates an example for estimating the vertical components of voltage gradient for a 27.7-cm sphere with profiles recorded at depths of 2, 5, 10, 20, 40, and 80 cm. Note how the three profiles plotted at depths of 2, 5, and 10 cm generate a common profile, and this uniformity indicates that there is no vertical gradient in this region of the electrical field. However, the graph shows an initial difference of about 35 volts between the profiles taken at depths 40 and 80 cm.

If it is assumed that this voltage is linearly applied over the 40 cm separating the two profiles (it is actually nonlinear), then the component of vertical gradient would be estimated at  $35 \text{ V}/40 \text{ cm} = 0.88 \text{ V/cm}$ . This magnitude of voltage gradient can be significant when electrofishing (Kolz and Reynolds 1989).

The voltage gradient probe (method 2) is well suited to measuring the horizontal components of voltage gradient. However, the probe illustrated in Fig. 11 cannot measure the components of ver-

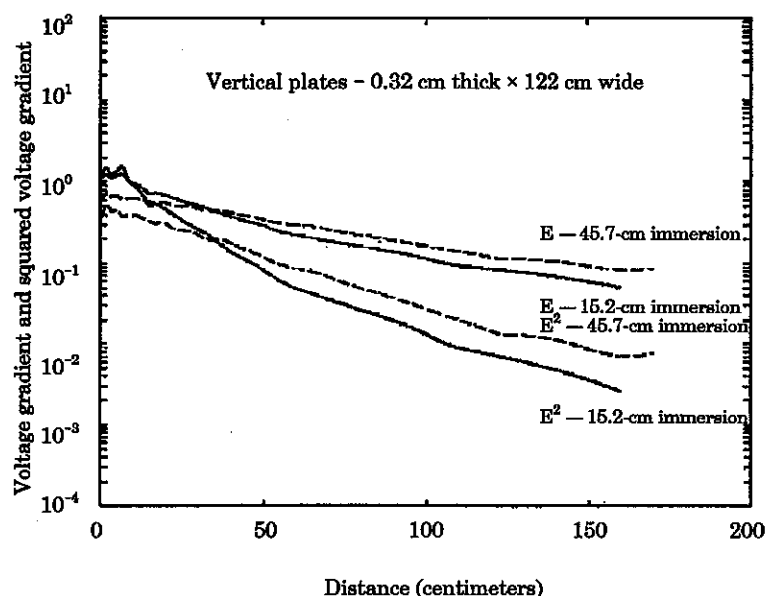


Fig. 23. Profiles of voltage gradient ( $E$ ) and the squared value of voltage gradient ( $E^2$ ) for two vertical plates measured along a transect normal to their surface.

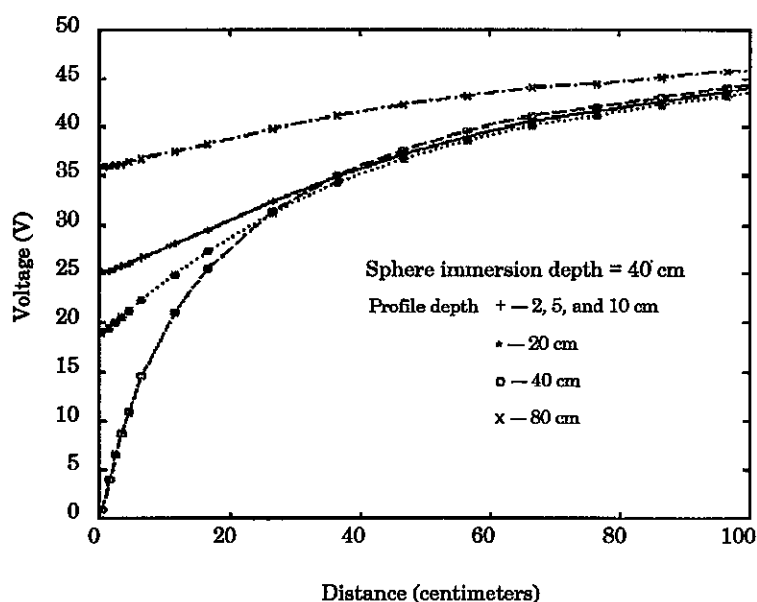


Fig. 24. Voltage profiles measured at six depths in the water on a common vertical plane to demonstrate the vertical components of voltage gradient for a 27.7-cm-diameter sphere.

tical gradient; it would be necessary to redesign the probe with additional sensors located in the vertical plane. Actually, electronic circuits could be developed to add the horizontal and vertical components and display the resultant magnitude of voltage gradient.

The electrofishing literature often describes the electroshock phenomenon by referring to the head-to-tail voltage (Edwards and Higgins 1973; Reynolds 1983; Jesien and Hocutt 1990; Zalewski and Cowx 1990). Since undisturbed fish are nor-

mally oriented horizontally in the water, it becomes easy to think of the horizontal component of voltage gradient as the head-to-tail voltage. However, fish rarely remain horizontal when subjected to an electrical shock, and all electrofishing systems produce electric fields with horizontal and vertical components of voltage gradient. In practice, the spatial direction and magnitude of the gradient vector must be considered to change continuously throughout the electric field. It becomes necessary to carefully differentiate as to



what is being defined as horizontal, vertical, head-to-tail, dorsal-to-ventral, or some other generalized description for voltage gradient.

The directional characteristic of the gradient vector becomes particularly significant when measuring the thresholds of electroshock response. Fish are most sensitive when their spinal columns are parallel to the voltage gradient vector (Lamarque 1990). This is not to imply that fish cannot be shocked in other orientations; in fact, fish can even be stunned in an electric field that effectively generates no head-to-tail voltage. There is little information regarding these directional effects, but one possible explanation (an unproven hypothesis) can be developed by applying Poynting's power vector (Ramo and Whinnery 1953). Under this concept, when the direction of electrical current flow is aligned with the spinal column, the power vectors are directed radially inward along the entire longitudinal axis of the fish (Fig. 25a). This orientation is optimal for the transfer and dissipation of power into the axis of the spinal column. Conversely, the least favorable orientation for power transfer occurs when the direction of electrical current is perpendicular to the spinal column (Fig. 25b). When transverse, there is less opportunity to transfer power because the vectors only intersect the width of the spinal column (rather than its entire length), and there is an additional reduction in the power transfer caused by the angular relation between the vectors and the spinal column.

## Discussion

The type of electrode configuration used for any particular electrofishing operation is dependent on a variety of electrical and biological factors. The guidelines for selecting an electrode design must include a knowledge of the following factors: power capabilities of the electrical source, desired size and intensity of the electric field, estimates of the thresholds of electroshock response for the fish to be sampled, how power density can be adjusted for changes in water conductivity, and special considerations regarding the working habitat (aquatic plants, poor water clarity, fast water, feeding areas, hazards, maneuverability, etc.). I described a generalized approach with appropriate measurement techniques to allow researchers to compare, measure, and adapt electrode designs to best accomplish a particular need. Remember—there is no such thing as the universally perfect electrode.

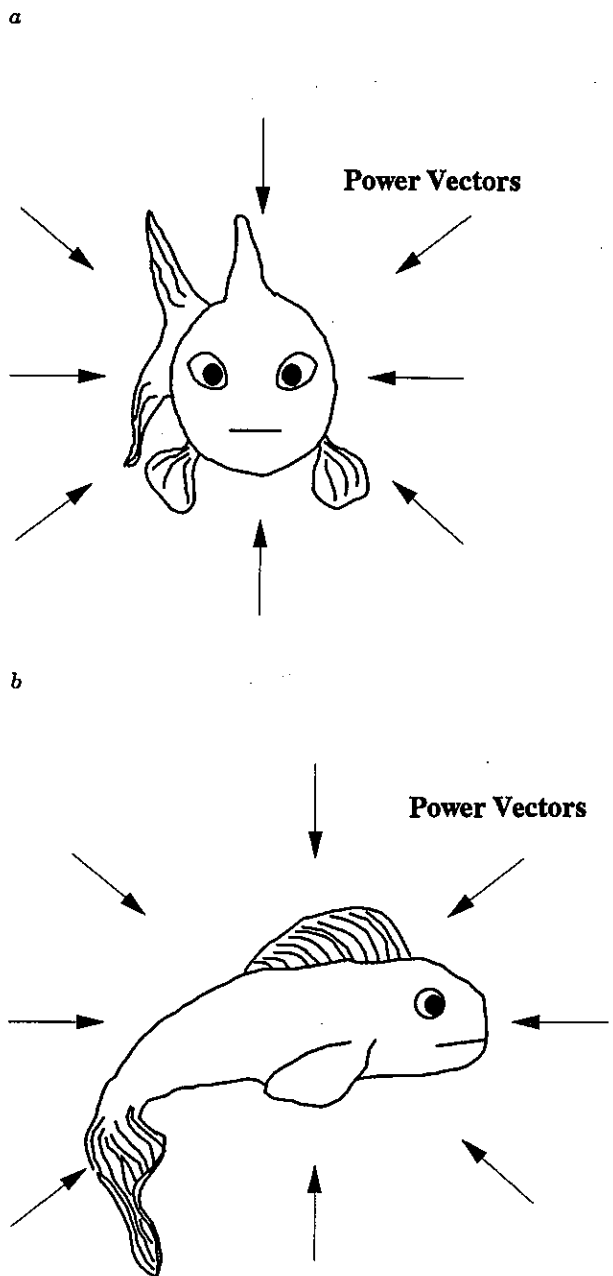


**Fig. 25.** Diagrams illustrate how power vectors intersect and transmit energy into the spinal column of a fish: (a) Power vectors intersect the entire length of the spinal column for a maximum transfer of energy when the spine is parallel to the direction of the electrical current. (b) Power vectors intersect only the width of the spinal column for a minimal transfer of energy when the spine is perpendicular to the direction of the electrical current.

The determination of an electrode's resistance and the development of the in-water voltage profiles

are crucial in the design of electrodes. These two characteristics allow the equipment designer to

1. calculate the total electrical resistance for any electrode array,
2. calculate the voltage distribution among the electrodes at any operating voltage and determine the individual and total electrode current,
3. calculate the system's total power requirement and determine the magnitude of the power dissipated at each electrode,
4. create graphic representations of the voltage profiles (S-curves),
5. create graphic representations of the voltage gradient profiles (U-curves),
6. compare the size of the in-water electric fields generated by different electrodes, and
7. comprehend the significance of power density and its relation to voltage gradient and water conductivity.

The success or failure of an electrofishing operation is often considered elusive and mystifying because the in-water electrical parameters are unknown or ignored. Unfortunately, a great deal of effort has been misdirected toward the metering of the electrical parameters at the power source. These on-board electrical measurements cannot be substituted for in-water measurements because the fish only respond to the stimuli in the water. Researchers will find electrofishing understandable only when they combine the information gathered through field observations of fish reacting to electroshock with a firm measurement basis of the in-water electrical parameters.

## Acknowledgments

I thank B. W. Mefford and T. J. Rhone of the Hydraulic Structures Section, U.S. Bureau of Reclamation, for their gracious consent and patience in allowing this research to be conducted at the hydraulics facility in Denver, Colo. Recognition is due S. A. Pruess of the Colorado School of Mines at Golden, Colo., for his guidance and assistance in the development of the computer codes necessary to perform the numerical analysis. The talents of D. K. Steffen created the computer artwork. The assistance of R. E. Johnson and F. A. Bush of the Denver Wildlife Research Center in laboratory setup and the collection of data is appreciated.

## References

- Brand, J. R. 1979. Handbook of electronics formulas, symbols and definitions. Van Nostrand Reinhold Company, Inc., New York. 359 pp.
- Conway, B. E. 1965. Theory and principles of electrode processes. The Ronald Press Company, New York. 303 pp.
- De Boor, C. W. 1978. A practical guide to splines. Springer Verlag, New York. 392 pp.
- DeMont, D. J. 1971. Physical factors affecting electrofishing in conductive waters. M.S. thesis, Humboldt State College, Arcata, Calif. 76 pp.
- Edwards, J. L., and J. D. Higgins. 1973. The effects of electric currents on fish. Final technical report, projects B-397, B-400 and E-200-301. Georgia Institute of Technology Engineering Experiment Station, Atlanta. 75 pp.
- Harris, A. T. 1955. A-C circuit analysis. McGraw-Hill Book Company, Inc., New York. 317 pp.
- Heidinger, R. C., D. R. Helms, T. I. Hiebert, and P. H. Howe. 1983. Operational comparison of three electrofishing systems. *North American Journal of Fisheries Management* 3:254-257.
- Jesien, R., and R. Hocutt. 1990. Method for evaluating fish response to electric fields. Pages 10-18 in I. G. Cowx, editor. *Developments in electric fishing*. Fishing News Books, Blackwell Scientific Publications Ltd., Oxford, England.
- Kolz, A. L. 1989. A power transfer theory for electrofishing. Pages 1-11 in *Electrofishing, a power related phenomenon*. U.S. Fish and Wildlife Service Fish and Wildlife Technical Report 22.
- Kolz, A. L., and J. B. Reynolds. 1989. Determination of power threshold response curves. Pages 15-24 in *Electrofishing, a power related phenomenon*. U.S. Fish and Wildlife Service Fish and Wildlife Technical Report 22.
- Lamarque, P. 1990. Electrophysiology of fish in electric fields. Pages 4-33 in I. G. Cowx and P. Lamarque, editors. *Fishing with electricity*. Fishing News Books, Blackwell Scientific Publications Ltd., Oxford, England.
- Novotny, D. W., and G. R. Priegel. 1974. Electrofishing boats: improved designs and operational guidelines to increase the effectiveness of boom shockers. Wisconsin Department of Natural Resources Technical Bulletin 73. 48 pp.
- Ramo, S., and J. R. Whinnery. 1953. Fields and waves in modern radio. 2nd edition. John Wiley & Sons, Inc., New York. 576 pp.
- Reynolds, J. B. 1983. Electrofishing. Pages 147-163 in L. A. Nielsen and D. L. Johnson, editors. *Fisheries techniques*. American Fisheries Society, Bethesda, Md.
- Rogers, W. E. 1954. Introduction to electric fields. McGraw-Hill Book Company, Inc., New York. 333 pp.
- Seidel, W. R., and E. F. Klima. 1974. In situ experiments with coastal pelagic fishes to establish design crite-

- ria for electrical fish harvesting systems. U.S. National Marine Fisheries Service Fishery Bulletin 72:657-669.
- Wiley, M. L., and C. Tsai. 1983. The relative efficiencies of electrofishing versus seines in Piedmont streams of Maryland. *North American Journal of Fisheries Management* 3:243-253.
- Zalewski, M., and I. G. Cowx. 1990. Factors affecting the efficiency of electric fishing. Pages 89-111 in I. G. Cowx and P. Lamarque, editors. *Fishing with electricity*. Fishing News Books, Blackwell Scientific Publications Ltd., Oxford, England.

## Appendix. Glossary of Electrical Terms

---

**Conductivity (c)** The ratio of the density of the unvarying current in a conductor to the voltage gradient that produces it. Common units of measurement are mhos per centimeter or siemens per centimeter (S/cm).

**Current (I)** The rate of electrical charge flow in a circuit. The practical unit is the ampere (1 coulomb/s).

**Electrical charge (Q)** A fundamental property of matter that can be classified as a fundamental physical quantity. The practical unit is the coulomb. The electron, the smallest charge identified in nature, has a magnitude of  $1.6 \times 10^{-19}$  coulomb.

**Power (P)** The rate of doing work or the energy per unit of time. The practical unit is the watt (1 joule/s).

**Power density (D)** The power or energy per unit of time dissipated in a given volume of

material. The unit of measurement is watts per cubic centimeter.

**Resistance (R)** The ability to react to the flow of AC or DC with an opposition to the flow of current. Also, the ratio of the applied voltage to the induced current that it produces. The unit of measurement is the ohm.

**Resistivity (r)** The reciprocal of conductivity. The common unit of measurement is the ohm-centimeter.

**Volts or voltage (V)** The energy per unit of electrical charge. The unit of measure is the volt (1 joule/coulomb).

**Voltage gradient (E)** The rate of change of voltage with distance. Also, the force per unit of electrical charge. The common unit of measurement is volts per centimeter.